remote sensing

MDPI

Article

Open Source Riverscapes: Analyzing the Corridor of the Naryn River in Kyrgyzstan Based on Open Access Data

Florian Betz *, Magdalena Lauermann and Bernd Cyffka

Catholic University Eichstaett-Ingolstadt, Applied Physical Geography, 85072 Eichstaett, Germany; magdalena.lauermann@ku.de (M.L.); bernd.cyffka@ku.de (B.C.)

* Correspondence: florian.betz@ku.de; Tel.: +49-8421-9323106

Received: 8 July 2020; Accepted: 5 August 2020; Published: 6 August 2020

Abstract: In fluvial geomorphology as well as in freshwater ecology, rivers are commonly seen as nested hierarchical systems functioning over a range of spatial and temporal scales. Thus, for a comprehensive assessment, information on various scales is required. Over the past decade, remote sensing-based approaches have become increasingly popular in river science to increase the spatial scale of analysis. However, data-scarce areas have been widely ignored so far, even if most remaining free flowing rivers are located in such areas. In this study, we suggest an approach for river corridor mapping based on open access data only, in order to foster large-scale analysis of river systems in data-scarce areas. We take the more than 600 km long Naryn River in Kyrgyzstan as an example, and demonstrate the potential of the SRTM-1 elevation model and Landsat OLI imagery in the automated mapping of various riverscape parameters, like the riparian zone extent, distribution of riparian vegetation, active channel width and confinement, as well as stream power. For each parameter, a rigor validation is performed to evaluate the performance of the applied datasets. The results demonstrate that our approach to riverscape mapping is capable of providing sufficiently accurate results for reach-averaged parameters, and is thus well-suited to large-scale river corridor assessment in data-scarce regions. Rather than an ultimate solution, we see this remote sensing approach as part of a multi-scale analysis framework with more detailed investigation in selected study reaches.

Keywords: riverscape; riparian zone; river management; remote sensing; open access data; Naryn River; Central Asia

1. Introduction

Rivers are increasingly under pressure worldwide due to anthropogenic activities like hydropower exploitation, and only very few free flowing rivers remain worldwide, most of them located in remote regions of the world [1,2]. Knowledge about these rivers is crucial in order to create a scientific basis for their protection. However, for most rivers in remote regions of the world, information remains sparse, limiting our capability to set up efficient monitoring schemes or create management plans [2]. Over the past years, progress in remote sensing technology has fostered the development of approaches to remote sensing-based analysis of river corridors [3–6]. Since becoming available, remote sensing has been used to overcome the issue of having only spatially loose sampling points along rivers, and create continuous data for entire river corridors or even networks. This spatially continuous view of rivers has become popular, under the label "riverscape" [7,8]. The remote sensing view of rivers allowed the testing of long-established theories of fluvial geomorphology and riverine ecology, such as the downstream hydraulic geometry [9] or the river continuum concept [10] and,

more recently, patch-oriented frameworks [11–13]. Results from remote sensing studies suggest that the structure of rivers is more complex, and is a result of multiple controlling factors (see for example Notebaert et al. [14], for a discussion). One consequence of this complex nature of river corridors is that the modern perspective on river science and management sees rivers as complex systems operating over a range of spatial and temporal scales. Thus, a comprehensive analysis of a particular river system requires well-planned investigations on multiple scales [15].

Over the past few years, the number of remote sensing studies in river science has increased [6,16]. In addition, tools like the fluvial corridor toolbox [17] have been developed to simplify the automated GIS analysis of river corridors. A clear focus of recent research in fluvial remote sensing has been on the use of high resolution data derived from LiDAR, aerial imagery or high resolution satellite sensors [18–20]. However, high resolution data is commonly unavailable for most remote areas, especially in a developing country context [21,22]. In addition, purchasing high resolution satellite imagery or organizing airborne surveys is limited by the high cost of data acquisition. This limits such studies to small river systems or single study reaches. As a consequence, the geomorphological and ecological structure of large river systems in remote areas tend to remain unexplored, at least from an up-to-date riverscape perspective. Today, only very few studies exist that make use of open access datasets in exploring the large-scale structure of river corridors. For instance, Schmitt et al. [21] used open access data along with auxiliary datasets to map the Mekong river system in Southeast Asia. Later, they extended this work to provide recommendations for sustainable sediment management [23]. From a European perspective, Clerici et al. [24] and Weissteiner et al. [25] used data freely available for the European Union to map floodplain ecosystems on a pan-European scale. They combined terrain analysis and multispectral remote sensing in a fuzzy logic approach, and were able to provide accurate information on this large spatial scale. However, they relies on auxiliary data and information not available beyond the European Union, such as standardized flood hazard maps or land cover information.

In this study, we take the Naryn River in Kyrgyzstan as an example, and present a framework for river corridor analysis based on terrain analysis and multispectral remote sensing using open access data only. The Naryn River is to date a free flowing river over a length of more than 600 km, forming a regional hotspot of biodiversity and providing manifold ecosystem services to local people. Despite this relevance, its geomorphological and ecological structure is still unexplored, apart from the previous studies of the authors of this study [22,26]. The aim of this study is to suggest a framework for river corridor analysis based on open access datasets only. With the results, we do not only fill the research gap for the Naryn River, but provide also methods for analyzing river corridors in other data-scarce regions of the world.

2. Study Area

The study area is the Naryn catchment in Kyrgyzstan upstream from the Toktogul reservoir (Figure 1c). The Naryn is a major tributary of the Syr Darya, and thus the uppermost headwater of the Aral Sea Basin (Figure 1c). The catchment upstream from the Toktogul has an entire area of 52,130 km^2, and the elevation ranges from 868 m at the outlet to 5133 m in the Tian Shan mountains (Figure 1d). Upstream from the Toktogul, the Naryn River is still in a widely natural condition without major dams or embankments, providing full longitudinal and lateral connectivity [22]. The climate is highly continental, with cold winters and hot summers (Figure 1b). The monthly temperatures range between −25 °C in January and +25 °C in August. With an average annual sum of 300 mm, the precipitation is in general low and has a clear season in May and June (Figure 1b). The discharge is dominated by snow- and glacier-melt in the Tian Shan mountains [27]. Consequently, the hydrograph shows a clear glacial regime with a single peak in July (Figure 1a).

The geological setting of the region is characterized by the active tectonics of the Tian Shan [28,29]. The consequence is an interplay of east–west striking mountain ranges and intramontane basins [29]. One of these is the Naryn Basin, located between Eki Naryn and Kazarman on Figure 1d. Within the

sediments of the basin, terraces have formed [29]. Where they are abundant, they form the ultimate boundary of the area connected to recent hydro-morphological processes of the Naryn River [22].

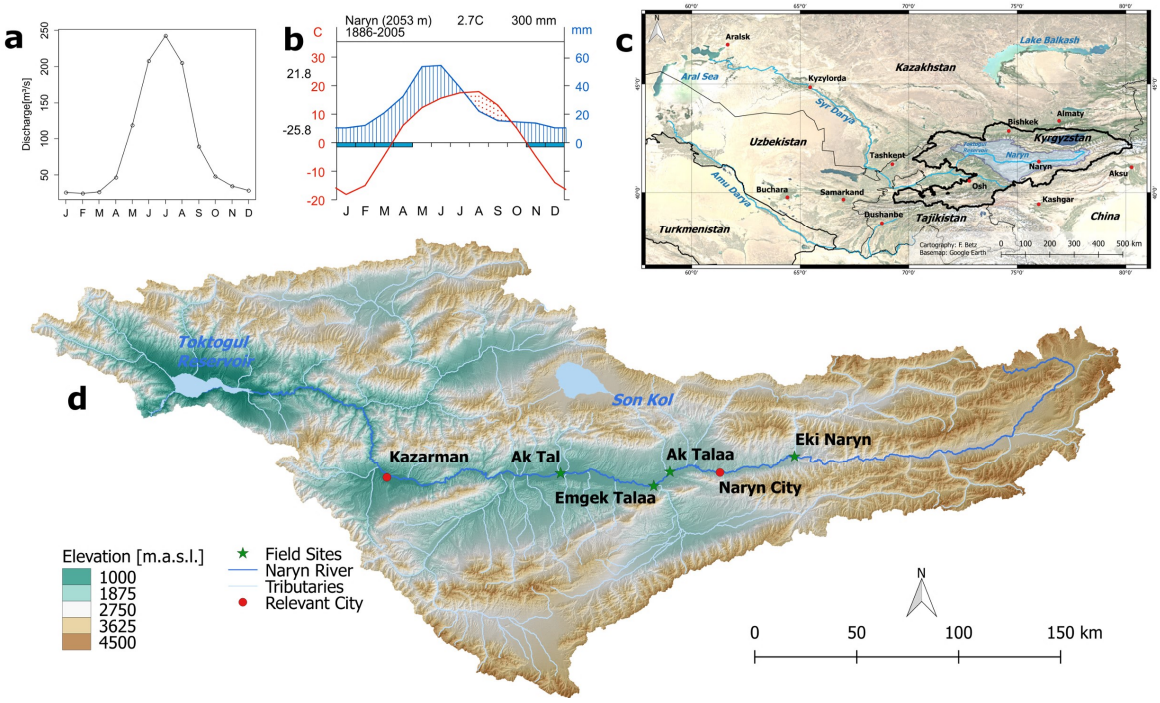

Figure 1. Overview over the study area: (**a**) hydrograph and (**b**) climate diagram of Naryn City; (**c**) location of the Naryn catchment within Central Asia and (**d**) detailed map of the catchment itself.

The riparian zone within these boundaries is structured into a braided plain flooded during the annual summer floods, and a floodplain inundated only during exceptional flood events. The vegetation developing on the highly dynamic braided plain is dominated by *Populus nigra*, *Salix talassica, Salix alba, Hippophae rhamnoides* and *Tamarix spp*. On the floodplains, species less resilient to inundation and hydraulic shear forces also occur, such as *Rosa spp.*, *Caragana spinosa* or *Berberis vulgaris*.

3. Data and Methods

3.1. An Open Access Approach to River Corridor Mapping

We use four main steps for mapping and analyzing the river corridor (Figure 2). Terrain analysis was used for creating the geomorphological template, i.e., for deriving the channel network, the associated river corridor and relevant controlling factors like stream power or confinement. Then, multispectral analysis was used to derive information about land cover, in our case riparian vegetation. In a fourth step, the spatial pattern of river corridor attributes was derived in a disaggregation/aggregation procedure, as suggested by Alber and Piégay [30]. In a final step, we carried out a spatial and statistical analysis for the various river corridor parameters derived from the previous steps.

Each river corridor is organized in a longitudinal and lateral way. For capturing the longitudinal perspective, the longitudinal profile and the channel gradient, as well as the discharge and total stream power, are estimated based on terrain analysis and discharge data from gauging stations. From the lateral perspective, the area belonging to the river corridor, the riparian zone, is characterized by its connectivity to the hydrological and geomorphological processes in the river channel, and is bounded by a blurred transition zone rather than by a sharp boundary [22,25,31]. To acknowledge this blurred character of the riparian zone boundary, we used a fuzzy logic-based approach for delineation, as suggested by Betz et al. [22]. Riparian vegetation is natural or semi-natural vegetation occurring within the riparian zone [31]. For assessing vegetation, multispectral remote sensing has

been established as the standard method. As anthropogenically modified areas like agriculture or forest plantations are absent in the vicinity of the Naryn River, we used a simple linear membership function of a vegetation index for assessment and combined it with the fuzzy riparian zone delineation to assess riparian vegetation. A more in-depth analysis of the vegetation is beyond the scope of this study. For other situations with more complex land cover in the riparian zone, more detailed classification approaches are needed (see, e.g., Weissteiner et al. [25]).

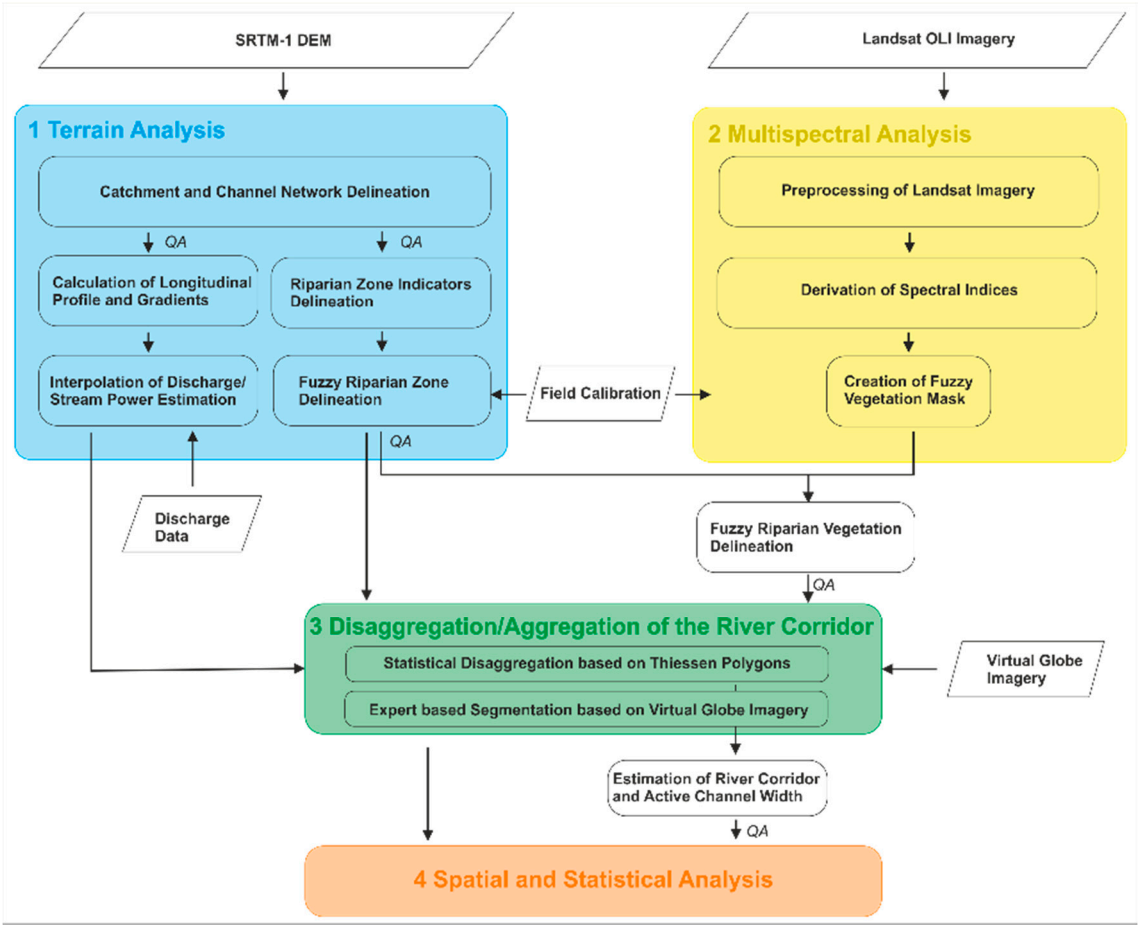

Figure 2. Workflow for riverscape analysis; QA stands for quality analysis.

The spatial structure of the river corridor was analyzed by means of a disaggregation/aggregation framework. First, we assessed the continuous information along the river, using the disaggregated 100 m segments. Then, the information was analyzed for the spatial units of reaches. The aggregation to reaches was performed based on river type mapping from high resolution virtual globe imagery. In this context, we defined a reach boundary as a change in river type [32]. In a final step, both longitudinally continuous information of the 100 m segments and reach-averaged information was combined in the multivariate statistical analysis of the river corridor of the Naryn River, in order to obtain a better large-scale understanding. All computations were carried out in R with an integration of GRASS GIS.

3.2. Data

For terrain analysis, we used the SRTM-1 DEM available at a resolution of 1 arcsecond, resulting in a pixel size of 24.05 × 24.05 m when projecting to UTM. To combine it with the multispectral imagery, the DEM was resampled to the resolution of the Landsat data (30 m). The vertical accuracy of this dataset is approximately 16 m [33]. For the multispectral analysis, Landsat OLI data from July 2015 was used. Landsat data is available on demand as surface reflectance data from the EROS

Science Processing Architecture on Demand Interface of the United States Geological Survey (USGS) (http://espa.cr.usug.gov). More details on the L8SR algorithm used by the USGS for converting the digital numbers of the satellite imagery to surface reflectance can be found in Vermote et al. [34]. In addition to the radiometric calibration, the USGS provides a cloud and cloud shadow mask, computed by the fmask algorithm [35,36]. As the methods applied by the USGS are highly sophisticated and can be considered to deliver a reliable output, no further pre-processing of the raw imagery was conducted [37]. Additionally, virtual globe imagery from various sources was used for the geomorphological classification of the river channel.

Besides the spatial data, discharge records of 18 gauges in the Naryn catchment were used for discharge interpolation and stream power estimation. This data is available online as monthly averages from the Northern Eurasian Earth Science Partnership Initiative (http://neespi.unh.edu).

3.3. Catchment, Channel Network Delineation and Longitudinal Profile

We used the *r.stream* toolkit implemented in GRASS GIS for the catchment and channel network delineation. This toolkit allows one to conduct flow routing through the unmodified DEM using a least cost path algorithm [38,39]. This approach has been proven to be more accurate compared to classical sink filling approaches [22,40]. In the first step, a flow accumulation grid was computed, and the channel network was extracted using a channel initiation threshold derived from channel heads digitized from Soviet military maps (see Lauermann et al. [41] for full details). Afterwards, the main stem of the Naryn River was extracted from this network using the Hack stream order.

The longitudinal profile is crucial for an analysis of river corridors, as it is used to derive the channel gradient and estimate stream power. It was derived from the elevation values and the cumulative distance along the computed channel line of the Naryn River. Coarse scale radar DEMs like SRTM-1 suffer from errors and noise [42]. Thus, we smoothed the original profile using a constrained quantile regression technique, as suggested by Schwanghart and Scherler [42]. The channel gradient was then calculated for each 100 m segment of the disaggregated channel line, based on the elevation difference between the first and the last elevation value per segment.

3.4. Discharge Interpolation and Stream Power Estimation

To compute spatially continuous values for the discharge, measured discharge values were correlated with the DEM-derived flow accumulation using a power law relationship of the form $a \times x^b$ [43]. The method of nonlinear least squares was used for determining the parameters a and b from the empirical data. The data for a total number of 18 gauges are available for the Naryn catchment. Commonly, the median annual flood (i.e., the flood with a 2 year return period) is used for the calculation of the stream power [44]. However, as only monthly discharge data is available in our study area, we used the median of the annual maxima, assuming that this is closer to the actual 2 year return period flood. This assumption is supported by tests with the gauge in Naryn City, where daily discharge data is available for the estimation of flood recurrence intervals.

The total stream power Ω [Wm^{-1}] is calculated from the channel gradient s, the unit weight of the water γ (9800 Nm^{-3}) and the discharge Q [m^3s^{-1}] [43,44]. The discharge can be substituted by the flow accumulation FA and the estimated regression coefficients a and b (Equation (1)).

$$\Omega = Q\gamma s = aFA^b\gamma s \quad (1)$$

3.5. Computation of Riparian Zone Indicators and Fuzzy Delineation of the Riparian Zone

For the riparian zone delineation, we used a fuzzy combination of the vertical distance to channel network (VDist), the modified topographic index (MTI) [45] and the multiresolution valley bottom flatness index (MRVBF) [46], as suggested by Betz et al. [22]. First, the indices were computed using modules available in GRASS GIS. Then, the index values were extracted at the locations of the field calibration sites. These calibration values were used to derive fuzzy membership functions.

We followed the suggestion of Weissteiner et al. [25], and used linear (Equation (2)) and inverse linear functions (Equation (3)).

$$\mu(x) = \begin{cases} 0 \; for \; x < x_{cal}(min) \\ \frac{x - x_{cal}(min)}{x_{cal}(max) - x_{cal}(min)} \quad for \; x\_cal(min) \leq x \leq x\_cal(max) \\ 1 \; for \; x > x\_cal(max) \end{cases} \tag{2}$$

$$\mu(x) = \begin{cases} 1 - \left(\frac{x}{x_{cal(max)}} \right) for \; x \leq x\_cal(max) \\ 0 \; for \; x > x\_cal(max) \end{cases} \tag{3}$$

In this equation, $x_{cal}(min)$ and $x_{cal}(max)$ are the minimum and the maximum value the respective indicator takes on the field calibration sites. Linear functions were developed for the MRVBF and the MTI, while an inverse linear function was used for the VDist. These membership functions have been applied to the entire Naryn catchment. Then, a fuzzy combination of all three indicator memberships was built using the fuzzy t-norm (fuzzy AND) and t-conorm (fuzzy OR). Semantically, we say "IF the vertical distance to channel network is low AND the MTI OR the MRVBF is high, THEN the membership degree to the riparian zone is high." We based our formulation on the classical formulation of Zadeh [47], and used the minimum for the fuzzy t-norm and the maximum for the fuzzy t-conorm to formalize this semantic formulation. Accordingly, we get the final riparian zone membership values for each grid cell of the elevation dataset of the Naryn catchment, according to Equation (4):

$$\mu_{final} = \min(\mu_{VDist}, \max(\mu_{MTI}, \; \mu_{MRVBF})) \tag{4}$$

In this equation, μ is the membership value of the respective parameter, e.g., μ_{VDist} is the membership of the vertical distance to channel network. Min and max refer to the minimum and the maximum of the membership value per grid cell. Grid cells with a membership value >0 are considered to be part of the riparian zone. For more details on the riparian zone delineation based on fuzzy membership functions, readers can refer to Betz et al. [22]. This reference includes, beyond a detailed technical description, an extensive evaluation of different morphometric indicators.

3.6. Landsat Preprocessing and Derivation of Spectral Indices

All bands of a total number of seven Landsat 8 OLI scenes, acquired in July 2015, have been mosaicked to cover the entire Naryn catchment. Clouds and cloud shadows have been masked out from further analysis using the Landsat quality band, which includes scores for clouds and cloud shadows computed by means of the fmask algorithm [35,36].

We used the tasseled cap angle as spectral index for vegetation delineation (Equation (5)):

$$TCA = \arctan\left(\frac{TCG}{TCB}\right) \tag{5}$$

TCA is the tasseled cap angle, *TCG* is the tasseled cap greenness and *TCB* is the tasseled cap brightness. The coefficients for the tasseled cap transformation of the Landsat OLI data have been taken from Baig et al. [48]. Full details on the tasseled cap angle can be found in Gomez et al. [49].

3.7. Fuzzy Vegetation Mask Creation and Derivation of Riparian Vegetation

The discrimination between vegetation and non-vegetation was conducted in a manner similar to the riparian zone delineation based on a fuzzy logic approach. A linear membership function (see Equation (2)) was constructed based on the tasseled cap angle. Riparian vegetation is defined as the vegetation within the riparian zone. Thus, the fuzzy intersection of the riparian zone membership and the vegetation membership was used to compute the riparian vegetation membership. If a pixel belongs to the class riparian zone and vegetation, then it is considered as riparian vegetation.

As suggested by Zadeh [47], we used the minimum of the intersection for computing this fuzzy AND rule (fuzzy t-norm).

3.8. Field Calibration

Field calibration is necessary for the fuzzy membership functions of riparian zone delineation and vegetation discrimination. It was carried out at three field sites across the central part of the Naryn catchment (Figure 1). These sites represent the major characteristics of the Naryn river corridor, from confined sites with narrow floodplains only to laterally unconfined sites with wide floodplains. A total number of 111 points were recorded in spring 2016 across different succession stages of the riparian vegetation. Then, the values of TCA, as well as of the different morphometric riparian zone indicators, were extracted for the sampling locations. The summary statistics of the extracted values have been computed to finally derive the values of x_{cal}(min) and x_{cal}(max), needed for the fuzzy membership functions. Table 1 summarizes the calibration values used in this study.

Table 1. Calibration values for the fuzzy membership functions obtained for the Naryn River.

Indicator	Function Type	X_{cal} (min)	X_{cal} (max)
Vertical Distance to channel network (VDist)	Inverse linear	-	6.65
Multiresolution Valley Bottom Flatness Index (MRVBF)	Linear	0.054	5.86
Modified Topographic Index (MTI)	Linear	2.03	11.61
Tasseled Cap Angle (TCA)	Linear	0.036	0.56

3.9. Disaggregation and Aggregation of the River Corridor

For the analysis of the river corridor structure, we followed Alber and Piégay [30], who suggested a disaggregation/aggregation framework. In the first step, the river corridor is disaggregated into segments of 100 m length (see Figure 3). These 100 m segments are a representation of longitudinally continuous data with a certain resolution. The resolution of the disaggregation depends on the dimension of the river and the spatial resolution of the input dataset. In this case, 100 m is considered to be an appropriate resolution, compared to the resolution of the input DEM and satellite imagery.

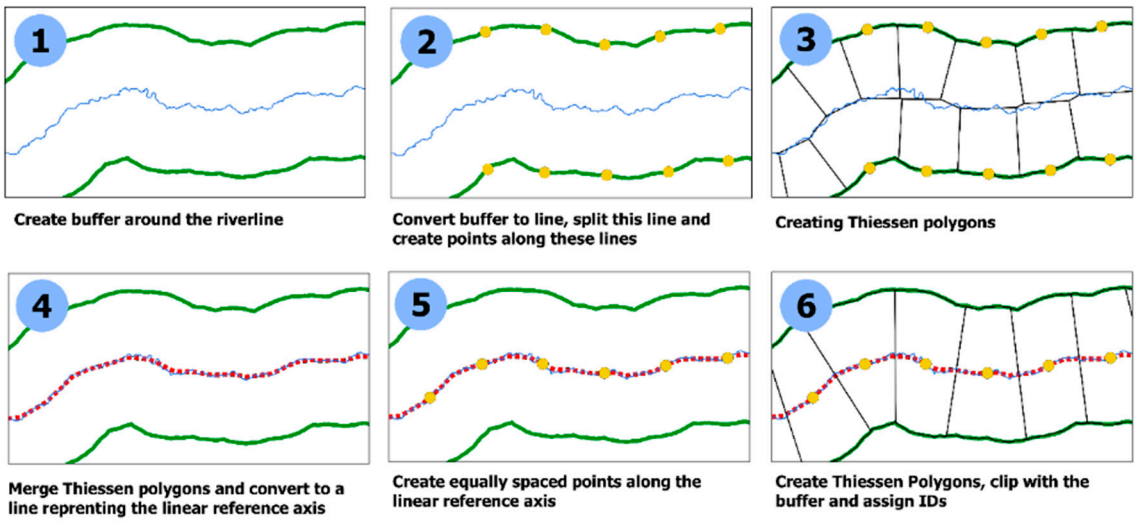

Figure 3. Framework for river corridor disaggregation (based on Alber and Piégay [30]); Please refer to the text for further explanation.

In the first step, the channel line was buffered by a distance wider than the expected maximal river corridor width. In the second step, the buffer was split into two lines, and points were generated at 100 m intervals along these lines. Then, Thiessen polygons were created from these points. Afterwards,

the Thiessen polygons were merged and converted into a line representing the linear reference axis of the river corridor. Again, points were generated along this line at 100 m intervals and used for Thiessen polygonization. These polygons were labeled with unique IDs. Now, information from the different raster datasets, such as the riparian vegetation extent, can be extracted for these polygons, and linked to the longitudinal profile via the unique ID.

While the disaggregation was used to generate longitudinally continuous information of river corridor parameters, the segmentation into reaches allowed a more process-based evaluation of the spatial structure of the Naryn River corridor. In this context, we defined a reach as a length of the river that operates under relatively consistent and characteristic boundary conditions [32]. While previous approaches to reach delineation focused on statistical approaches, such as spatially constrained clustering or change point detection methods [50–52], we used planform characteristics mapped from high resolution virtual globe images, whereby a reach boundary is defined by a change in the planform. We based the planform mapping upon the *Riverstyles* framework [32,53], and the distinguishing attributes of the different planform types of the Naryn River are given in Table 2.

Table 2. River types and their distinguishing attributes used for channel planform mapping.

Specification	Distinguishing Attribute
Reservoir	wide channel with anthropogenic margins
Gorge	bedrock confined valley setting with narrow channel
Straight	low sinuosity with no extensive instream features and absent or discontinuous floodplains
Braided	low sinuosity with extended gravel bars or islands, clearly identifiable main channel
Braided–Anastomosing	low sinuosity with multiple channels; single channels show characteristics of braided rivers with extended bars and islands
Steep Headwater	low sinuosity with confined valley setting; instream geomorphic features like bars or islands as well as floodplains are widely absent

3.10. Width Estimation and Confinement Assessment Based on the Disaggregated River Corridor

The values of river corridor and active channel width are relevant parameters of the riverscape. Their estimation is based on the disaggregated 100 m segments. Assuming that each of the segments is approximately rectangular, there is a close relationship between the area and the width as the length along the river line is fixed at 100 m. For the river corridor width, we simply used the area of the riparian zone as derived by the fuzzy riparian zone delineation. The active channel is defined as the part of the river corridor inundated during bankfull discharge. In practice, the absence of vegetation is used as indicator [21]. The unvegetated fraction in each 100 m segment was obtained from the fuzzy riparian vegetation delineation, based on multispectral remote sensing. As initial tests revealed that a straightforward calculation by dividing the area by 100 m was not suitable, we used this as an indicator for a width prediction based on measured river corridor and active channel width. A total number of 150 points has been generated along the channel line of the Naryn River where the Strahler order has been used as stratification. The number of points per Strahler order was determined by the percentage of length the segment with the order contributes to the total length of the river. We used 100 of the width measurements at these points for the linear regression of the areas derived from the fuzzy riparian zone and vegetation delineation, and the point measurements. The remaining 50 points were used as an independent validation dataset (see Section on quality assessment). Based on the width estimations, the confinement ratio (CR) can be calculated as the ratio of the active channel width and the river corridor width. If this index is close to 1, the river segment is likely to be confined, while an index close to 0 indicates a laterally unconfined situation [54]. Previous work has suggested that the CR is well suited to indicate channel confinement on large spatial scales [21].

3.11. Quality Assessment

At several points of the workflow, quality assessment was implemented to analyze the accuracy of the results. First, the accuracy of the derived Naryn River channel was tested by using the distances to a river line that has been digitized based on high resolution imagery. This method has already been used by Lauermann et al. [41] and Betz et al. [22]. A second quality assessment was performed for the fuzzy delineation of the riparian zone and riparian vegetation. Here, we followed the approach of Clerici et al. [24] and used the visual interpretation of high resolution virtual globe imagery for the validation of the riparian zone membership [22]. For the validation of the riparian vegetation delineation, the acquisition date of the image matters; thus virtual globe imagery was not feasible for this task. Instead, we used a true color Rapid Eye image from a date close to the acquisition date of the Landsat imagery for the visual discrimination of vegetation and no-vegetation. A total number of 250 points was randomly generated within a 1500 m wide buffer around the channel line of the Naryn River. For each point, it was evaluated whether it belongs to the riparian zone or not and whether it is vegetated or not. For the evaluation of the fuzzy riparian zone mask and the fuzzy vegetation mask, all membership values >0 were regarded as belonging to a respective class, that is to say, low membership values were also included. For a quantitative accuracy assessment, the user's and producer's accuracy were computed. An overall accuracy value is not meaningful for rare land cover classes like riparian zone or riparian vegetation [24]. In addition, the 95% confidence intervals of the accuracy values were computed following the approach of Olofsson et al. [55]. Finally, the estimation of river corridor and active channel width was validated against independent measurements based on high resolution satellite imagery provided by virtual globes. The R^2 of the modeled versus the measured widths was used as a quality indicator for the derived active channel and the river corridor width.

4. Results and Implications for the Structure of the Naryn River Corridor

4.1. Catchment, Channel Network and Longitudinal Profile

The first results from terrain analysis are the catchment delineation, resulting in the total catchment and the channel network. The catchment has a total area of 52,130 km^2, with an elevation ranging from 868 m at the Toktugul to 5133 m in the Tian Shan mountains. Considering the Naryn River and its main tributaries, the entire river network has a length of 4872 km. The main stem (Hack order 1) of the Naryn River has a length of 754 km from the uppermost headwaters to the Toktogul dam. A map of the catchment as well as the river network is presented in Figure 1 in the study area section. The quality assessment of the DEM-derived channel line shows good agreement with the course of the digitized river line; no relevant structure was missed. The median deviation of 30.8 m mainly arises from situations where the digitizing followed the thalweg of the river, which was not correctly represented in the DEM.

The longitudinal profile is shown in Figure 4, including the profile from the raw elevation values and a profile smoothed by means of a constrained quantile regression. In addition, it includes the channel gradient derived from the smoothed profile.

Already from the raw profile, it is obvious that there are several clearly identifiable knickpoints, especially in the upper part of the Naryn River. However, the errors and noise of the raw profile also become obvious. The blue line in Figure 4 shows the profile smoothed by means of a constrained quantile regression. This algorithm was able to remove errors, such as the spikes at approximately 500 km as well as noise, while preserving real knickpoints. In addition, continuously decreasing downstream values are ensured. The absolute residuals between raw and smoothed elevation have been calculated as a measure of profile modification. The average absolute residual is 3.3 m, indicating that the overall modification of the profile by the smoothing algorithm is relatively small. The maximum absolute residual is 205.25 m, reached at the spikes at 500 km profile distance. However, as no benchmark DEM is available (e.g., from LiDAR data), no independent evaluation of the longitudinal profile is possible. Nevertheless, the visual assessment of the smoothed profile shows a plausible

pattern, with removed noise and spikes and preserved knickpoints. Thus, we consider the resulting profile as a realistic representation of the longitudinal profile of the Naryn River. The channel gradients indicated in light grey in Figure 4 range from 0.06 mm^{-1} in the uppermost section of the Naryn to a gradient of 0 mm^{-1} in the Toktogul reservoir. The average gradient is 0.042 mm^{-1}. In general, the channel gradient tends to decrease from the uppermost headwaters towards the Toktogul reservoir. However, the spatial pattern is heterogeneous and does not follow a clear trend.

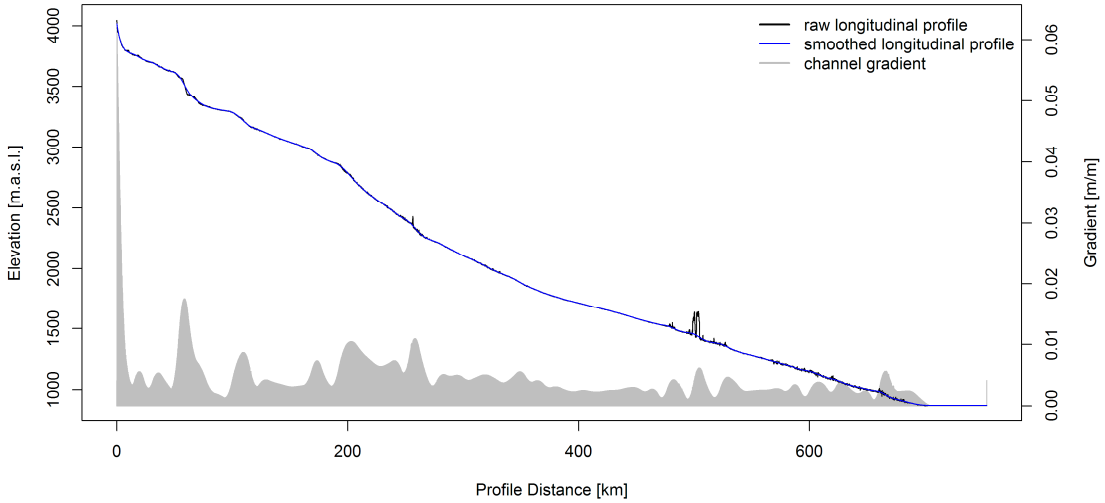

Figure 4. Longitudinal profile of the Naryn River based on the original elevation values (black line) and values smoothed by means of a constrained quantile regression (blue line); additionally, the channel gradient derived from the smoothed elevation values is shown in light grey.

Figure 5 shows the estimation of the channel gradient, interpolated discharge and the total stream power. The continuous discharge values arise from the power law relationship between the DEM-derived flow accumulation (FA) and the annual maxima of 18 gauging stations. The nonlinear least square fitting resulted in the equation $Q = 0.0009757 \times FA^{7375}$. The evaluation of the fitting procedure by means of a residual analysis reveals that this equation describes well the relationship between discharge and FA. Thus, the discharge estimation can be considered to be reliable.

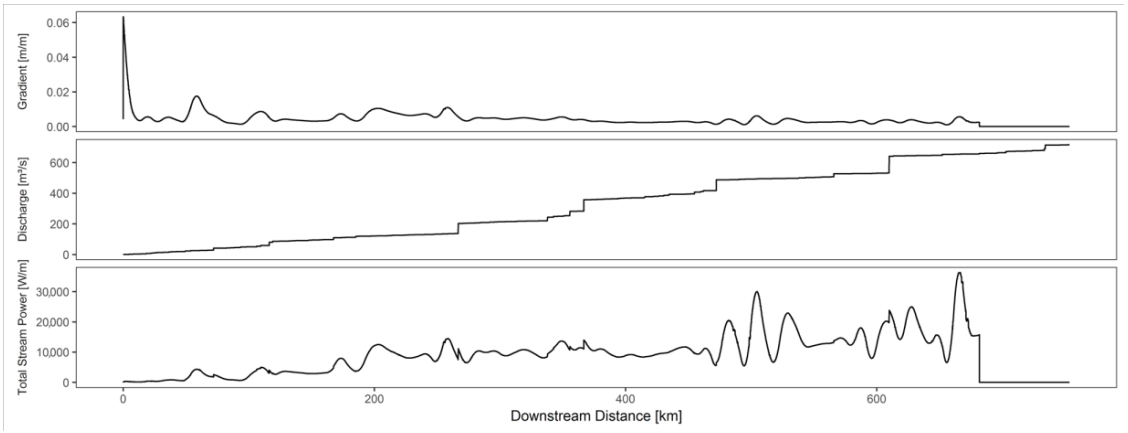

Figure 5. Channel gradients, discharge interpolation and total stream power along the longitudinal profile; the steps in the discharge curve arise from tributaries flowing into the Naryn River and causing a sudden increase in the discharge.

In general, stream power tends to increase following the general trend of increasing discharge. On the other hand, the heterogeneous channel gradients lead to a high degree of heterogeneity in the stream power.

4.2. Riparian Zone and Riparian Vegetation

The fuzzy derivation of the riparian zone along the Naryn River, performed by a combination of the vertical distance to the channel network, the modified topographic index and the multiresolution valley bottom flatness index, results in a user's accuracy of 82.14 ± 7.51%, while the producer's accuracy yields a value of 91.09 ± 5.58%. The producer's and user's accuracy of the riparian vegetation classification are 93.94 ± 4.7% and 85.19 ± 13.4%, respectively. The high uncertainty of the user's accuracy mainly arises from the low number of validation points within the riparian zone. More details on the riparian zone delineation can be found in Betz et al. [22].

The entire riparian zone has an area of 662.58 km^2. This area includes the Toktogul reservoir, with an area of 229 km^2. Thus, the area in which we can assume natural riparian dynamics is 443.58 km^2, including the active channel, instream geomorphic features such as bars or islands, and the floodplain. The distribution is not homogeneous along the Naryn River (Figure 6). In the uppermost part of the catchment, near the village of Kara Say, there is already a large patch of riparian zone with an area of 67.47 km^2. Around Ak Tal, the largest patch is found, with a riparian zone area of 97.83 km^2 and a vegetation area of 62.21 km^2. This patch already contributes 26.86% of the entire riparian vegetation along the Naryn River. The patch around Kazarman has a riparian zone extent of 42.99 km^2, with a vegetated area of 31.28 km^2. Downstream from Kazarman, the Naryn River enters a section characterized by a narrow river corridor and the absence of riparian vegetation. Downstream from this section, the river enters the Toktogul reservoir. While there is a fringe of vegetation around the reservoir, this is not considered as natural riparian vegetation due to the anthropogenic impact on the river and its floodplain.

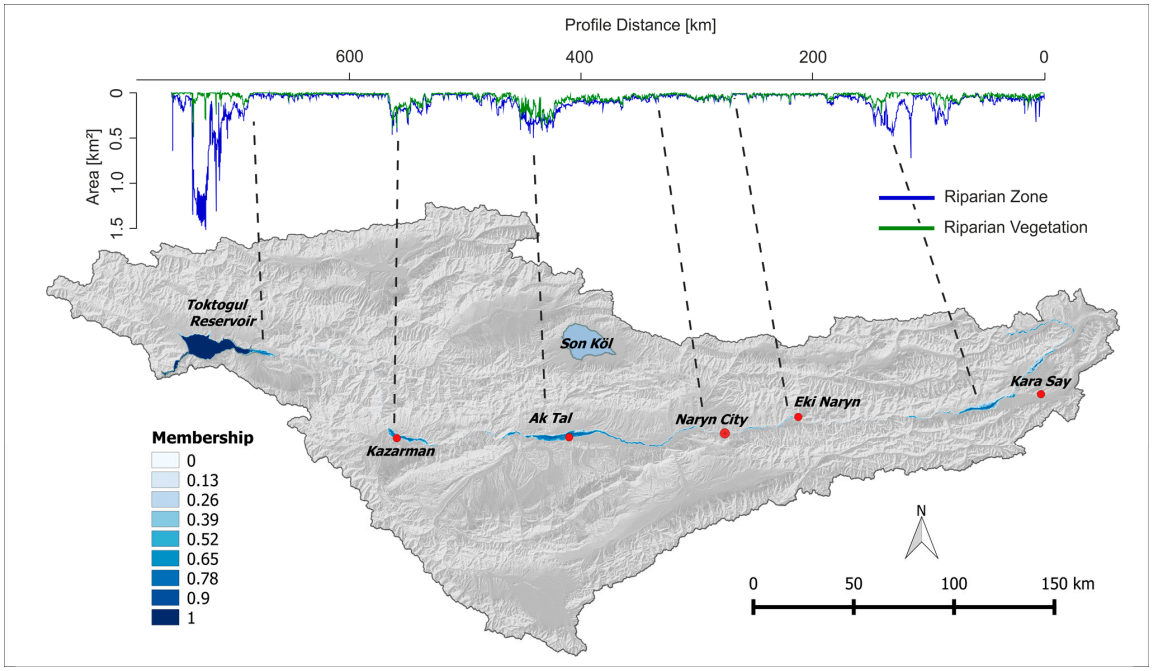

Figure 6. Riparian zone and riparian vegetation along the Naryn River; the map indicates the riparian zone only, while the longitudinal plot gives the area of the riparian zone in blue as well as the area of riparian vegetation in green.

4.3. Width Estimation and Confinement

Figure 7 shows the width estimation as well as the confinement ratio along the longitudinal profile of the Naryn River. The pattern reflects the general structure already visible in the distribution of the riparian zone.

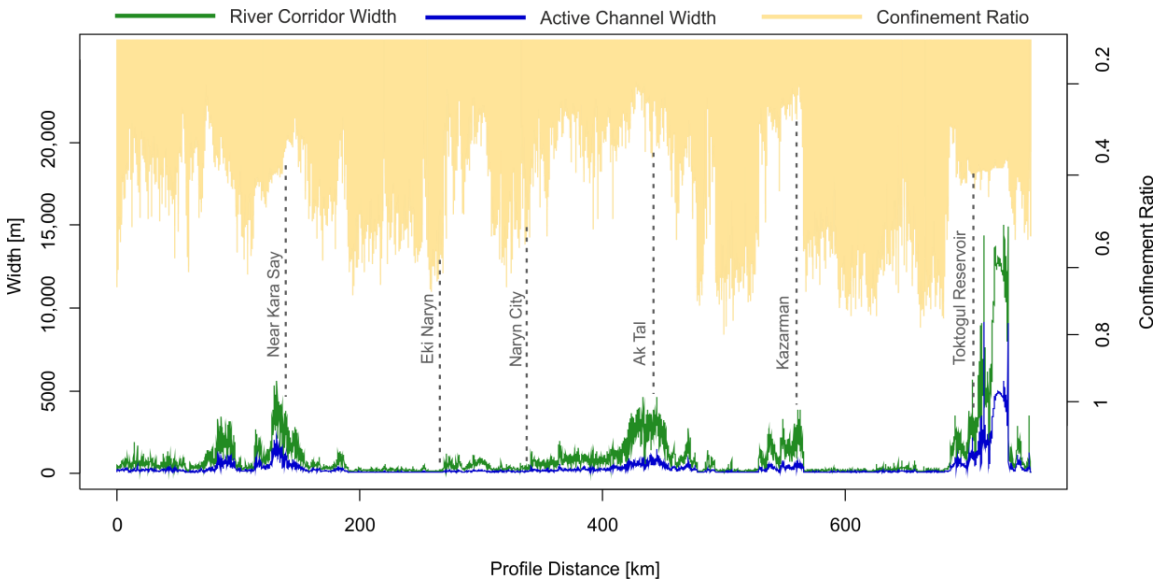

Figure 7. River corridor (green line) and active channel width (blue line); the confinement ratio is shown in yellow.

The majority of the Naryn River tends to be narrow, with an average width of 769 m and an average active channel width of 248 m. However, there are several wider sections, like the one near Kara Say with a width of 1957.7 m, and at Ak Tal and Kazarman, where the corridor width is up to 4648 m and the active channel width up to 3886 m. Not surprisingly, the Toktogul reservoir is the widest part of the river, with a width of 5149 m. The confinement ratio follows the general pattern of the river corridor and active channel width. In the wider sections near Kara Say, Ak Tal and Kazarman, low values of the ratio, ranging from 0.1455 to 0.49, indicate laterally unconfined river sections. On the contrary, river sections, e.g., between Ak Tal and Kazarman, or right upstream from the Toktogul reservoir, show high values of confinement ratio with values up to 0.7464, indicating confined conditions. In an overall evaluation, the Naryn River tends to show a certain degree of confinement, with an average confinement ratio value of 0.3995. However, the pattern is patchy and heterogeneous over the flow length.

Validating the results of the width estimation of the river corridor and the active channel yields R^2-values of 0.952 and 0.84, respectively. The uncertainty of the active channel width estimation is clearly associated with channel sections with more than 500 m widths, where our approach tends to underestimate channel width. Nevertheless, the methods yields values sufficiently accurate for the scale of interest in this study.

4.4. Segmentation of the River Corridor

The segmentation of the Naryn River corridor is based on the river type mapping results for a total number of 121 reaches, where a reach boundary is defined as a change in the river type (Figure 8). In the uppermost part upstream from Eki Naryn, steep headwaters are the dominating planform, even if shorter sections, classified as braided river, occur as well. Between Eki Naryn and Naryn City, an interplay of straight and braided river sections characterizes the river corridor. Downstream from Naryn City, the braided river sections become longer, while around Ak Tal even braided–anastomosing reaches are abundant. Between Ak Tal and Kazarman, the braided and braided–anastomosing reaches are interrupted by a gorge. Downstream from Kazarman, a long gorge leads towards the Toktogul reservoir.

In the overall evaluation, braided reaches are the dominant river type in the Naryn River, representing 211.3 km or 28.12% of the entire Naryn River. In addition, gorges with a total length of 174.57 km (23.16%) and steep headwaters (167 km or 22.21%) are relevant river types. The three

remaining river types make up a considerably smaller portion of the river corridor. The Toktogul reservoir contributes 9.53%, and straight reaches 10.24%. A special case is the braided–anastomosing reaches, which differ from braided reaches by the abundance of multiple channels clearly separated by vegetated floodplain patches. This particular river type has an entire length of 49.12 km, contributing 6.52% of the entire flow length of the Naryn River. While braided reaches are found along almost the entire Naryn River, braided–anastomosing reaches occur only around Ak Tal and Kazarman.

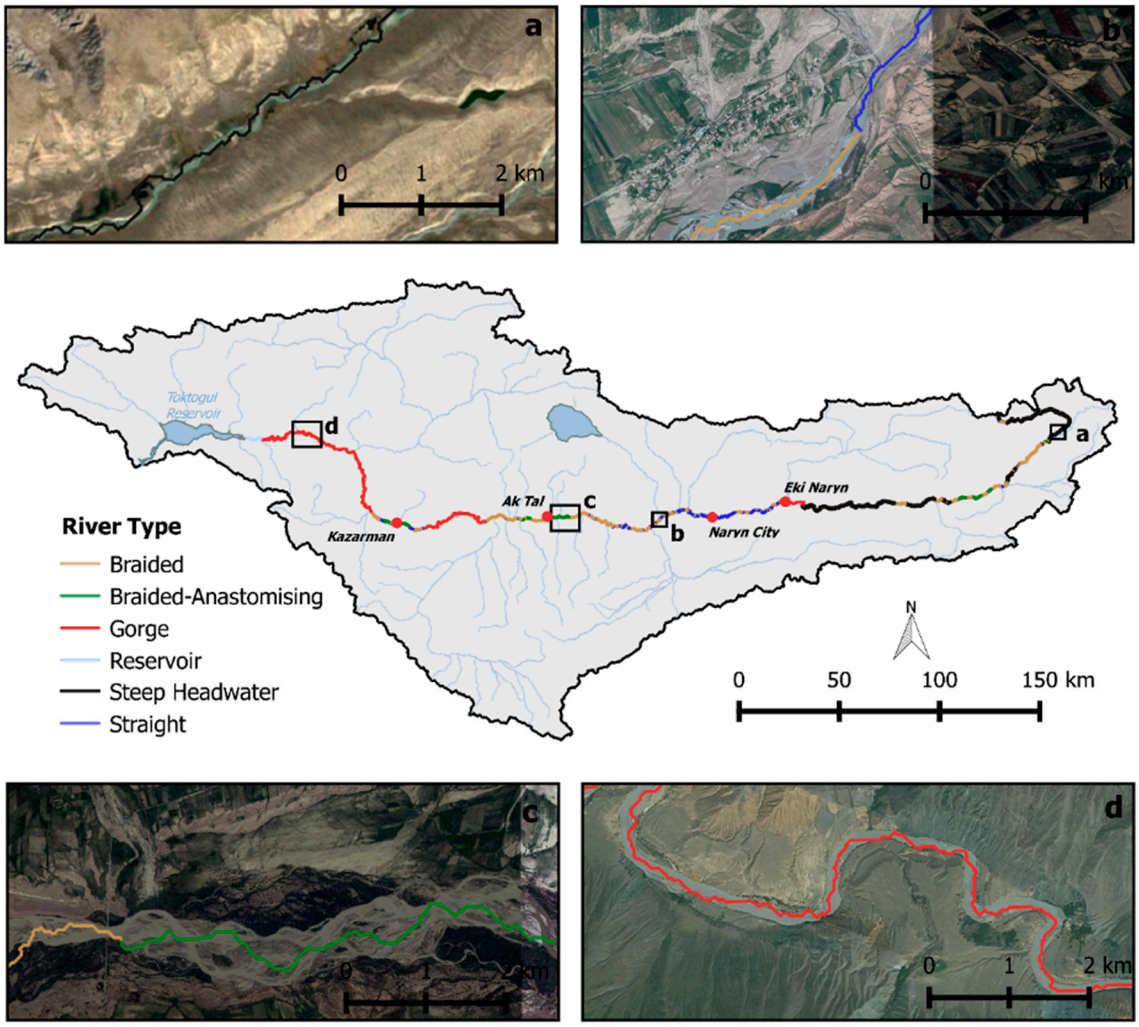

Figure 8. Results of the planform mapping based on virtual globe imagery; the insets (**a**–**d**) show detailed examples of the most relevant river types.

4.5. Spatial Analysis of the River Corridor

First, we test whether there is any longitudinal scaling of river corridor attributes, by means of a spearman correlation between the downstream distance and the various attributes. Three parameters show a certain degree of correlation: channel gradient (rho = −0.56), and total (rho = 0.84) as well as specific stream power (rho = 0.65). All other parameters do not show a clear relation with downstream distance, indicating that there is no longitudinal scaling. This indicates that the Naryn River is organized in a rather patchy way, as is manifested also in the alternating organization of the river types (Figure 8). This supports the conceptual view of rivers being organized in the form of distinct hydrogeomorphic patches, rather than in a longitudinal continuum [11,13].

Within the river types, there are clear differences regarding the different corridor parameters (Figure 9). The corridors tend to be widest in reaches with braided and braided–anastomosing planforms, with median values of 910 m and 2185 m, respectively. The other river types tend to have

much smaller widths. Straight reaches have a median corridor width of 440 m, steep headwaters 341 m and the gorges 195 m. This difference is also reflected in the channel gradient, where the steep headwaters are steepest, with a median gradient of 0.006707 mm^{-1} followed by the straight reaches with 0.004521 mm^{-1}, and the braided reaches have a median gradient of 0.003036 mm^{-1}. Braided–anastomosing reaches and gorges tend to have the lowest channel gradients, of 0.0030 mm^{-1} and 0.002799 mm^{-1}, respectively.

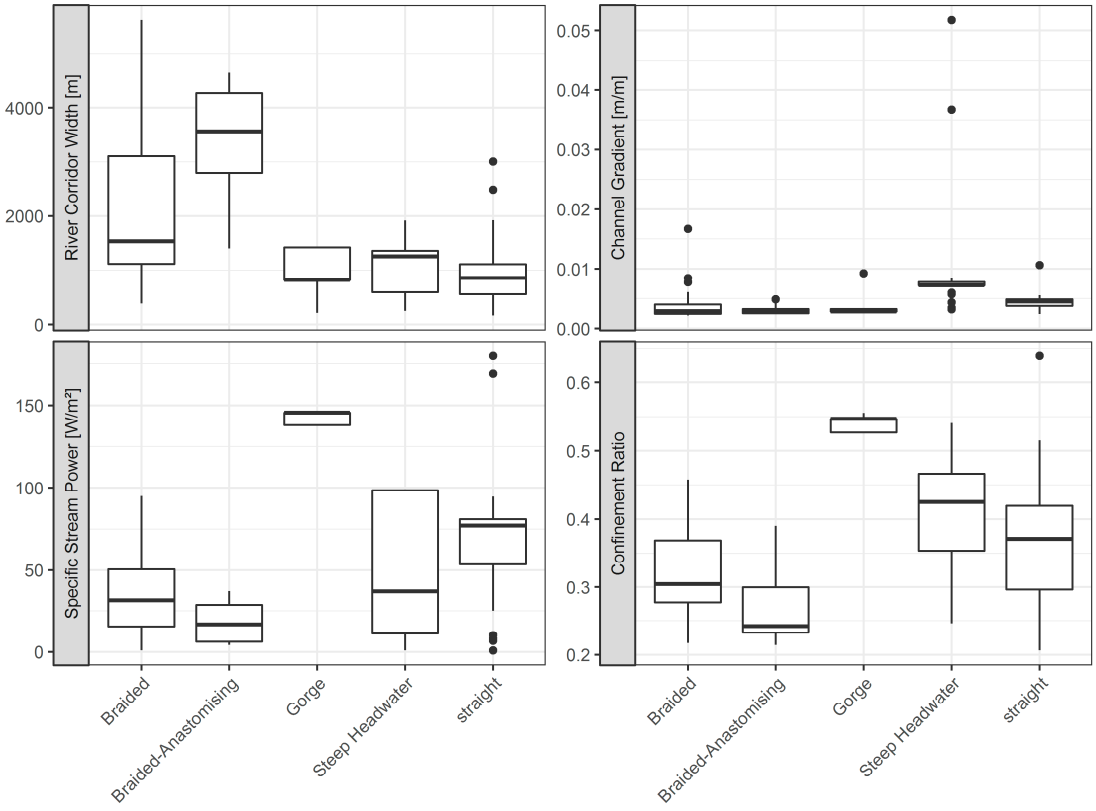

Figure 9. River corridor parameters for the different river types; the reservoir has been avoided for this figure to enhance readability.

Despite the high channel gradient, the median value of specific stream power is only 30.8 Wm^{-2} for the steep headwaters, while the gorges have the highest values of 138.9 Wm^{-2}, followed by the straight reaches with 70.6 Wm^{-2}. However, the variability of the stream power of the headwaters is considerably high, reflecting a certain heterogeneity in this river type. Braided and braided–anastomosing reaches have the lowest specific stream power values, of 27.7 Wm^{-2} and 15.7 Wm^{-2}, respectively. The difference among the different river types is probably most obvious in the confinement ratio. Here, the median values of the gorges (0.56) indicate a clearly confined situation, while the values of steep headwaters (0.42) and straight reaches (0.35) are smaller, and show a higher variability. The confinement ratios of braided and braided–anastomosing reaches are much smaller, with median values of 0.31 and 0.25. These river types tend to be laterally unconfined or partly confined.

The different characteristics of the river types are also reflected in the distribution of the riparian zone area and the area of riparian vegetation (Figure 10). The reservoir already contributes a high amount of the riparian zone (39%). For the natural reaches, braided and braided–anastomosing reaches dominate, with portions of 34.5% and 14%. The remaining area is distributed among the straight reaches, gorges and steep headwaters. With 175 km of river length characterized as gorge, this river type is an important feature of the Naryn River. However, due to the median width of 195.5 m only, the area of riparian zone is rather small for this river type. Most of the riparian vegetation is located within the braided (99.5 km^2) and braided–anastomosing reaches (52.4 km^2). Another 28.7 km^2 are located

in the steep headwaters. The remaining area of riparian vegetation is spread over small floodplain pockets within the straight reaches (22.8 km^2) and the gorges (10.4 km^2). The vegetation at the margin of the Toktogul reservoir (17.6 km^2) is not considered as natural riparian vegetation.

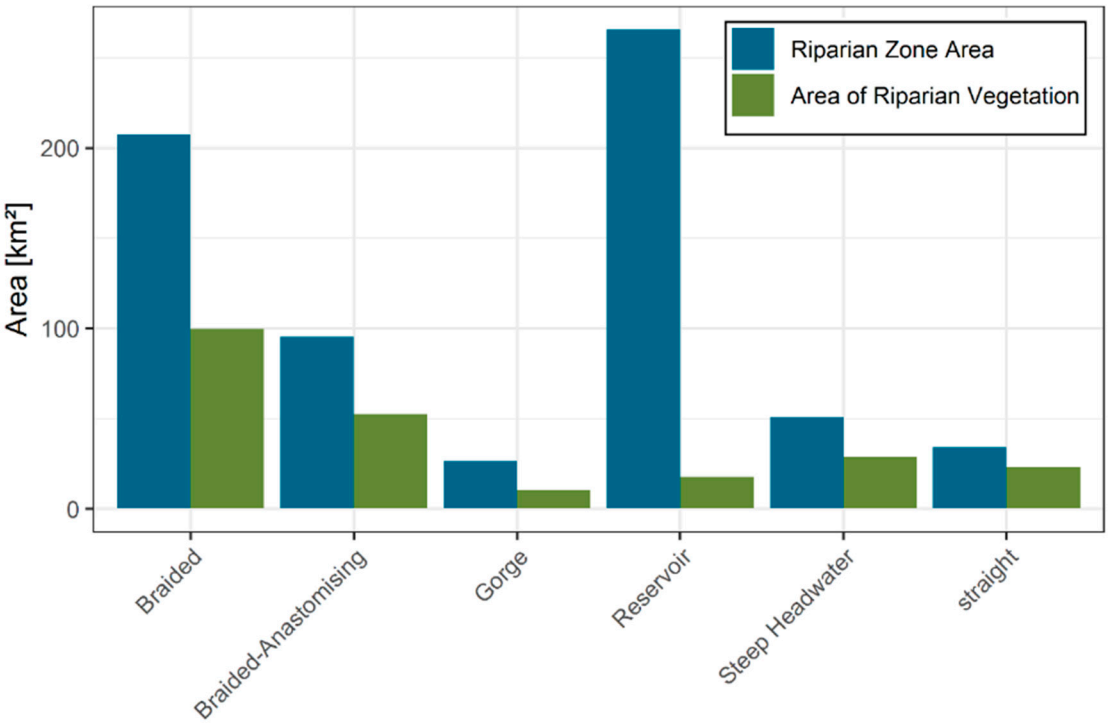

Figure 10. Riparian zone and riparian vegetation per river type; vegetation occurring along the Toktogul reservoir is not considered as natural riparian vegetation.

Now we have seen that there are clear differences among the different river types. What, though, controls the formation of these types? As there manifold highly intercorrelated parameters, a principal component analysis has been carried out to answer these questions (Figure 11). The river types are mainly arranged along the axis of confinement–river corridor width (CR - R_Width in the figure). Channel gradient and specific stream power seem to have only a minor influence.

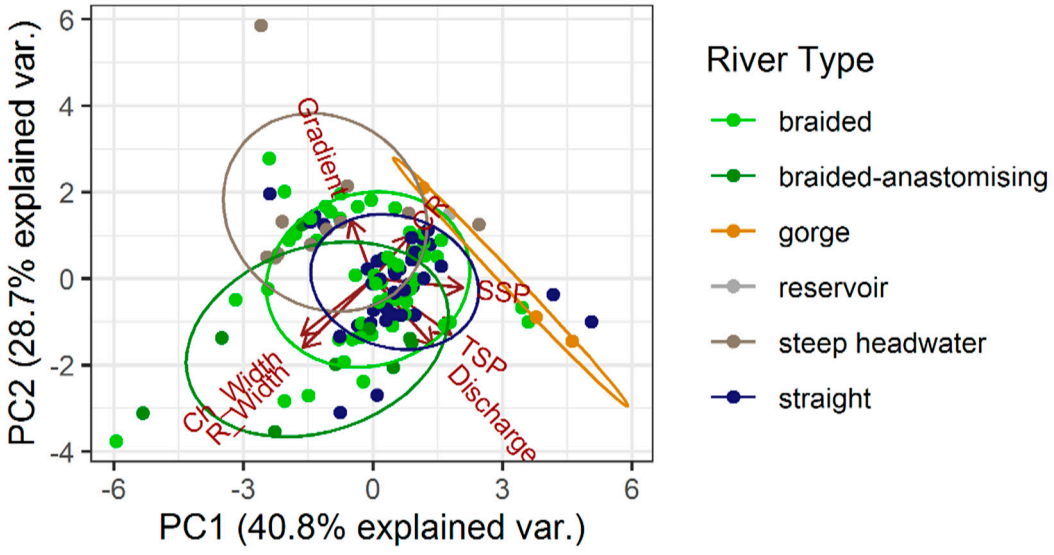

Figure 11. Principle component analysis for the river types and the different river corridor parameters.

Thus, confinement is considered to be the primary controlling factor of planform development for the Naryn River. In cases where the river has enough space to develop, braided and braided–anastomosing planforms develop, along with extended patches of riparian vegetation. In these reaches, we expect a certain interaction of vegetation and planform development, while in the confined reaches geological constraints are assumed to be the major control of river development. This combination of geological control and recent geomorphological forces shaping rivers is a widely recognized phenomenon, and has already been extensively discussed in the literature [56,57]. The results for the Naryn River clearly show the strong control of geological history over river planform development. Thus, the hypothesis of geological history controlling recent hydromorphological processes can be considered as true for the Naryn River.

5. Discussion

From a conceptual perspective, the analysis of rivers across multiple scales is relevant for a sound understanding of their functioning [3,15,58]. Despite the fact that this conceptual view is commonly accepted by the river science community, large-scale studies are just recently arising due to advances in remote sensing [6,16]. Despite the overall progress in remote sensing and the increasing availability of open access datasets, tests of these datasets in fluvial remote sensing are still limited [21,22].

We use the case of the Naryn River in Kyrgyzstan, and demonstrate the derivation of geomorphological and ecological information for this river using a combination of terrain analysis (SRTM-1 DEM) and multispectral remote sensing (Landsat 8 OLI). In contrast to Clerici et al. [24] and Weissteiner et al. [25], who present a detailed landcover mapping of the riparian zone, we rely only upon a minimum of field calibration data, and no further auxiliary datasets. This makes our approach suitable for remote regions of the world, where often no auxiliary data is available and the possibility for field data collection is limited. As we rely on open access data only, this makes our approach applicable to large-scale studies in remote regions of the world, an issue which has not been extensively studied before [6]. The accuracy assessment shows that our mapping approach using open access data along with a minimum input of field calibration is capable of delivering a realistic representation of a range of riverscape parameters. These parameters include more simple ones, like the channel line or longitudinal profile, but also more complex ones like active channel width or specific stream power. Compared to previous studies [21,44], the assessment of the lateral dimension of the river corridor in particular could be improved by the fuzzy logic-based assessment of the riparian zone, and the derivation of the active channel and river corridor width for each 100 m segment. However, the spatial resolution of the input data limits the degree of detail of the derived information. We see the results presented in this study as averages of the spatial scales of the disaggregated 100 m segments and the expert-derived reaches. Thus, elements of the river corridor with a finer spatial scale, such as single geomorphological units (e.g., single bars or islands), are not considered to be individually contrary to high resolution remote sensing studies [18]. As a consequence, the results of our open access approach are suitable for a characterization of rivers on the scale of entire river networks, into corridors or individual segments. Information on these scales is relevant to analyzing the structure of the river system and defining the study reaches or sampling sites [15,58]. Other applications might include large-scale planning in a developing country context [23]. On finer scales, open access remote sensing, as presented in this study, is very limited, due to the spatial resolution of the input datasets, and data with higher spatial resolution, such as high resolution satellite imagery, drone surveys or field sampling, might be necessary to deliver more detailed information [4].

6. Conclusions

In this study, we present an open access approach to river corridor analysis based on the example of the Naryn River in Kyrgyzstan. This approach allows the derivation of a wide range of parameters, with an accuracy suitable for the large-scale characterization of river corridors. This allowed the data-driven analysis of the more than 600 km long Naryn River, and generated the first quantitative

information about its large-scale geomorphological and ecological structure. This data reveals that the Naryn is primarily controlled by the geological structure of the region. Only in the central part of the catchment, where the valley is wide enough to allow the development of a laterally unconfined river corridor, stream power is a relevant formative agent in river planform and riparian vegetation development. Of course, our results do not allow an in-depth analysis of single river reaches, due to the spatial resolution and accuracy of the open access input data. However, the information on the scale of an entire river corridor, or potentially entire river networks, allows the strategic selection of study sites for more detailed investigation. In the case of the Naryn River, we suggest the selection of the braided and braided–anastomosing reaches between Naryn City and Kazarman, especially the reach around the village of Ak Tal, for more detailed investigation, as the wide river corridor, with an extensive braided plain and floodplain covered by a mosaic of riparian vegetation, is promising for studying the dynamics of a river that currently still has a natural flow regime with full lateral and longitudinal connectivity. All in all, we conclude that open access digital elevation data and multispectral satellite imagery, along with appropriate methods and rigor accuracy assessment, are well suited for deriving quantitative information for large river corridors from data-scarce regions. However, rather than a final information product, we see our remote sensing-based investigation as part of a multiscale framework that should also include more detailed analysis in well-selected sections within a river network.

Author Contributions: Conceptualization, F.B.; methodology, F.B.; validation, F.B. and M.L.; formal analysis, F.B. and M.L.; writing—original draft preparation, F.B.; writing—review and editing, M.L. and B.C.; visualization, F.B. and M.L.; supervision, B.C.; funding acquisition, B.C. All authors have read and agreed to the published version of the manuscript.

Funding: This research was founded by the Volkswagen Foundation (grant no. 88497) and the Federal Ministry of Education and Research (grant no. 01LZ1802A). The open access publication of this article was supported by the Open Access Fund of the Catholic University Eichstaett-Ingolstadt.

Conflicts of Interest: The authors declare no conflict of interest.

References

1. Zarfl, C.; Lumsdon, A.E.; Berlekamp, J.; Tydecks, L.; Tockner, K. A global boom in hydropower dam construction. *Aquat. Sci.* **2015**, *77*, 161–170. [CrossRef]
2. Grill, G.; Lehner, B.; Thieme, M.; Geenen, B.; Tickner, D.; Antonelli, F.; Babu, S.; Borrelli, P.; Cheng, L.; Crochetiere, H.; et al. Mapping the world's free-flowing rivers. *Nature* **2019**, *569*, 215–221. [CrossRef] [PubMed]
3. Carbonneau, P.; Piégay, H. *Fluvial Remote Sensing for Science and Management*; Wiley-Blackwell: Oxford, UK, 2012.
4. Piégay, H.; Arnaud, F.; Belletti, B.; Bertrand, M.; Bizzi, S.; Carbonneau, P.; Dufour, S.; Liebault, F.; Ruiz-Villanueva, V.; Slater, L. Remotely Sensed Rivers in the Anthropocene: State of the Art and Prospects. *Earth Surf. Process. Landf.* **2019**. [CrossRef]
5. Fryirs, K.A.; Wheaton, J.M.; Bizzi, S.; Williams, R.; Brierley, G.J. To plug-in or not to plug-in? Geomorphic analysis of rivers using the River Styles Framework in an era of big data acquisition and automation. *Wiley Interdiscip. Rev. Water* **2019**, *321*, 146. [CrossRef]
6. Tomsett, C.; Leyland, J. Remote sensing of river corridors: A review of current trends and future directions. *River Res. Appl.* **2019**, *45*, 19. [CrossRef]
7. Fonstad, M.A.; Andrew Marcus, W. High resolution, basin extent observations and implications for understanding river form and process. *Earth Surf. Process. Landf.* **2010**, *35*, 680–698. [CrossRef]
8. Carbonneau, P.; Fonstad, M.A.; Marcus, W.A.; Dugdale, S.J. Making riverscapes real. *Geomorphology* **2012**, *137*, 74–86. [CrossRef]
9. Leopold, L.B.; Maddock, T. *The Hydraulic Geometry of Stream Channels and Some Physiographic Implications*; Quantitative measurement of some of the hydraulic factors that help to determine the shape of natural stream channels: Depth, width, velocity, and suspended load, and how they vary with discharge as simple power functions. Their interrelations are described by the term "hydraulic geometry"; U.S. Government Printing Office: Washington, DC, USA, 1953.

10. Vannote, R.L.; Minshall, W.; Cummins, K.W.; Sedell, J.R.; Cushing, C.E. The River Continuum Concept. *Can. J. Fish. Aquat. Sci.* **1980**, *37*, 130–137. [CrossRef]
11. Poole, G.C. Fluvial landscape ecology: Addressing uniqueness within the river discontinuum. *Freshw. Biol.* **2002**, *47*, 641–660. [CrossRef]
12. Ward, J.V.; Tockner, K.; Arscott, D.B.; Claret, C. Riverine landscape diversity. *Freshw. Biol.* **2002**, *47*, 517–539. [CrossRef]
13. Thorp, J.H.; Thoms, M.C.; Delong, M.D. The riverine ecosystem synthesis: Biocomplexity in river networks across space and time. *River Res. Appl.* **2006**, *22*, 123–147. [CrossRef]
14. Notebaert, B.; Piégay, H. Multi-scale factors controlling the pattern of floodplain width at a network scale: The case of the Rhône basin, France. *Geomorphology* **2013**, *200*, 155–171. [CrossRef]
15. Gurnell, A.M.; Rinaldi, M.; Belletti, B.; Bizzi, S.; Blamauer, B.; Braca, G.; Buijse, A.D.; Bussettini, M.; Camenen, B.; Comiti, F.; et al. A multi-scale hierarchical framework for developing understanding of river behaviour to support river management. *Aquat. Sci.* **2016**, *78*, 1–16. [CrossRef]
16. Bizzi, S.; Demarchi, L.; Grabowski, R.C.; Weissteiner, C.J.; van de Bund, W. The use of remote sensing to characterise hydromorphological properties of European rivers. *Aquat. Sci.* **2016**, *78*, 57–70. [CrossRef]
17. Roux, C.; Alber, A.; Bertrand, M.; Vaudor, L.; Piégay, H. "FluvialCorridor": A new ArcGIS toolbox package for multiscale riverscape exploration. *Geomorphology* **2015**, *242*, 29–37. [CrossRef]
18. Demarchi, L.; Bizzi, S.; Piégay, H. Regional hydromorphological characterization with continuous and automated remote sensing analysis based on VHR imagery and low-resolution LiDAR data. *Earth Surf. Process. Landf.* **2016**, *42*, 531–551. [CrossRef]
19. Bizzi, S.; Piégay, H.; Demarchi, L.; van de Bund, W.; Weissteiner, C.J.; Gob, F. LiDAR-based fluvial remote sensing to assess 50–100-year human-driven channel changes at a regional level: The case of the Piedmont Region, Italy. *Earth Surf. Process. Landf.* **2019**, *44*, 471–489. [CrossRef]
20. Michez, A.; Piégay, H.; Lejeune, P.; Claessens, H. Multi-temporal monitoring of a regional riparian buffer network (>12,000 km) with LiDAR and photogrammetric point clouds. *J. Environ. Manag.* **2017**, *202*, 424–436. [CrossRef]
21. Schmitt, R.; Bizzi, S.; Castelletti, A. Characterizing fluvial systems at basin scale by fuzzy signatures of hydromorphological drivers in data scarce environments. *Geomorphology* **2014**, *214*, 69–83. [CrossRef]
22. Betz, F.; Lauermann, M.; Cyffka, B. Delineation of the riparian zone in data-scarce regions using fuzzy membership functions: An evaluation based on the case of the Naryn River in Kyrgyzstan. *Geomorphology* **2018**, *306*, 170–181. [CrossRef]
23. Schmitt, R.J.P.; Bizzi, S.; Castelletti, A.; Kondolf, G.M. Improved trade-offs of hydropower and sand connectivity by strategic dam planning in the Mekong. *Nat. Sustain.* **2018**, *1*, 96–104. [CrossRef]
24. Clerici, N.; Weissteiner, C.J.; Paracchini, M.L.; Boschetti, L.; Baraldi, A.; Strobl, P. Pan-European distribution modelling of stream riparian zones based on multi-source Earth Observation data. *Ecol. Indic.* **2013**, *24*, 211–223. [CrossRef]
25. Weissteiner, C.; Ickerott, M.; Ott, H.; Probeck, M.; Ramminger, G.; Clerici, N.; Dufourmont, H.; Sousa, A.D. Europe's Green Arteries—A Continental Dataset of Riparian Zones. *Remote Sens.* **2016**, *8*, 925. [CrossRef]
26. Betz, F.; Rauschenberger, J.; Lauermann, M.; Cyffka, B. Using GIS and Remote Sensing for Assessing Riparian Ecosystems along the Naryn River, Kyrgyzstan. *Int. J. Geoinform.* **2016**, *12*, 25–30.
27. Kriegel, D.; Mayer, C.; Hagg, W.; Vorogushyn, S.; Duethmann, D.; Gafurov, A.; Farinotti, D. Changes in glacierisation, climate and runoff in the second half of the 20th century in the Naryn basin, Central Asia. *Glob. Planet. Chang.* **2013**, *110*, 51–61. [CrossRef]
28. de Grave, J.; Glorie, S.; Ryabinin, A.; Zhimulev, F.; Buslov, M.M.; Izmer, A.; Elburg, M.; Vanhaecke, F.; Van den Haute, P. Late Palaeozoic and Meso-Cenozoic tectonic evolution of the southern Kyrgyz Tien Shan: Constraints from multi-method thermochronology in the Trans-Alai, Turkestan-Alai segment and the southeastern Ferghana Basin. *J. Asian Earth Sci.* **2012**, *44*, 149–168. [CrossRef]
29. Thompson, S.C.; Weldon, R.J.; Rubin, C.M.; Abdrakhmatov, K.; Molnar, P.; Berger, G.W. Late Quaternary slip rates across the central Tien Shan, Kyrgyzstan, central Asia. *J. Geophys. Res.* **2002**, *107*, ETG 7-1–ETG 7-32. [CrossRef]
30. Alber, A.; Piégay, H. Spatial disaggregation and aggregation procedures for characterizing fluvial features at the network-scale: Application to the Rhône basin (France). *Geomorphology* **2011**, *125*, 343–360. [CrossRef]

31. Naiman, R.J.; Décamps, H.; McClain, M.E. *Riparia: Ecology, Conservation and Management of Streamside Communities*; Elsevier Academics: Amsterdam, The Netherlands, 2005.
32. Fryirs, K.A.; Brierley, G.J. *Geomorphic Analysis of River Systems: An Approach to Reading the Landscape*, 1st ed.; Wiley-Blackwell: Oxford, UK, 2013; ISBN 978-1-4051-9275-0.
33. Farr, T.G.; Rosen, P.A.; Caro, E.; Crippen, R.; Duren, R.; Hensley, S.; Kobrick, M.; Paller, M.; Rodriguez, E.; Roth, L.; et al. The Shuttle Radar Topography Mission. *Rev. Geophys.* **2007**, *45*, RG2004. [CrossRef]
34. Vermote, E.; Justice, C.; Claverie, M.; Franch, B. Preliminary analysis of the performance of the Landsat 8/OLI land surface reflectance product. *Remote Sens. Environ.* **2016**, *185*, 46–56. [CrossRef]
35. Zhu, Z.; Woodcock, C.E. Object-based cloud and cloud shadow detection in Landsat imagery. *Remote Sens. Environ.* **2012**, *118*, 83–94. [CrossRef]
36. Zhu, Z.; Wang, S.; Woodcock, C.E. Improvement and expansion of the Fmask algorithm: Cloud, cloud shadow, and snow detection for Landsats 4–7, 8, and Sentinel 2 images. *Remote Sens. Environ.* **2015**, *159*, 269–277. [CrossRef]
37. Young, N.E.; Anderson, R.S.; Chignell, S.M.; Vorster, A.G.; Lawrence, R.; Evangelista, P.H. A survival guide to Landsat preprocessing. *Ecology* **2017**, *98*, 920–932. [CrossRef] [PubMed]
38. Jasiewicz, J.; Metz, M. A new GRASS GIS toolkit for Hortonian analysis of drainage networks. *Comput. Geosci.* **2011**, *37*, 1162–1173. [CrossRef]
39. Metz, M.; Mitasova, H.; Harmon, R.S. Efficient extraction of drainage networks from massive, radar-based elevation models with least cost path search. *Hydrol. Earth Syst. Sci.* **2011**, *15*, 667–678. [CrossRef]
40. Metz, M.; Mitasova, H.; Harmon, R.S. Accurate stream extraction from large, radar-based elevation models. *Hydrol. Earth Syst. Sci. Discuss.* **2010**, *7*, 3213–3235. [CrossRef]
41. Lauermann, M.; Betz, F.; Cyffka, B. *Channel Network Derivation from Digital Elevation Models—An Evaluation of Open Source Approaches*; Conference Paper; Catholic University Eichstätt-Ingolstadt: Eichstätt, Germany, 2016.
42. Schwanghart, W.; Scherler, D. Bumps in river profiles: Uncertainty assessment and smoothing using quantile regression techniques. *Earth Surf. Dyn.* **2017**, *5*, 821–839. [CrossRef]
43. Knighton, A.D. Downstream variation in stream power. *Geomorphology* **1999**, *29*, 293–306. [CrossRef]
44. Bizzi, S.; Lerner, D.N. The Use of Stream Power as an Indicator of Channel Sensitivity to Erosion and Deposition Processes. *River Res. Appl.* **2015**, *31*, 16–27. [CrossRef]
45. Manfreda, S.; Sole, A.; Fiorentino, M. Can the basin morphology alone provide an insight into floodplain delineation? *WIT Trans. Ecol. Environ.* **2008**, *118*, 47–56. [CrossRef]
46. Gallant, J.C.; Dowling, T.I. A multiresolution index of valley bottom flatness for mapping depositional areas. *Water Resour. Res.* **2003**, *39*. [CrossRef]
47. Zadeh, L.A. Fuzzy sets. *Inf. Control* **1965**, *8*, 338–353. [CrossRef]
48. Baig, M.H.A.; Zhang, L.; Shuai, T.; Tong, Q. Derivation of a tasseled cap transformation based on Landsat 8 at-satellite reflectance. *Int. J. Remote Sens.* **2014**, *5*, 423–431. [CrossRef]
49. Gómez, C.; White, J.C.; Wulder, M.A. Characterizing the state and processes of change in a dynamic forest environment using hierarchical spatio-temporal segmentation. *Remote Sens. Environ.* **2011**, *115*, 1665–1679. [CrossRef]
50. Leviandier, T.; Alber, A.; Le Ber, F.; Piégay, H. Comparison of statistical algorithms for detecting homogeneous river reaches along a longitudinal continuum. *Geomorphology* **2012**, *138*, 130–144. [CrossRef]
51. Parker, C.; Clifford, N.J.; Thorne, C.R. Automatic delineation of functional river reach boundaries for river research and applications. *River Res. Appl.* **2012**, *28*, 1708–1725. [CrossRef]
52. Martínez-Fernández, V.; Solana-Gutiérrez, J.; González del Tánago, M.; García de Jalón, D. Automatic procedures for river reach delineation: Univariate and multivariate approaches in a fluvial context. *Geomorphology* **2016**, *253*, 38–47. [CrossRef]
53. Brierley, G.J.; Fryirs, K.A. *Geomorphology and River Management: Applications of the River Styles Framework*, 1st ed.; Wiley-Blackwell Publishing: Malden, MA, USA, 2005; ISBN 1-4051-1516-5.
54. Nicoll, T.J.; Hickin, E.J. Planform geometry and channel migration of confined meandering rivers on the Canadian prairies. *Geomorphology* **2010**, *116*, 37–47. [CrossRef]
55. Olofsson, P.; Foody, G.M.; Herold, M.; Stehman, S.V.; Woodcock, C.E.; Wulder, M.A. Good practices for estimating area and assessing accuracy of land change. *Remote Sens. Environ.* **2014**, *148*, 42–57. [CrossRef]
56. Phillips, J.D. The perfect landscape. *Geomorphology* **2007**, *84*, 159–169. [CrossRef]

57. Fryirs, K.A. River sensitivity: A lost foundation concept in fluvial geomorphology. *Earth Surf. Process. Landf.* **2017**, *42*, 55–70. [CrossRef]
58. Fausch, K.D.; Torgersen, C.E.; Baxter, C.V.; Li, H.W. Landscapes to Riverscapes: Bridging the Gap between Research and Conservation of Stream Fishes. *BioScience* **2002**, *52*, 483–498. [CrossRef]